JOURNAL OF MATERIALS SCIENCE 39 (2004) 1331–1335

Characterization and coating properties of silsesquioxanes derived from the hydrolytic condensation of (3-glycidoxypropyl)trimethoxysilane

LIJIANG HU*‡, XINGWEN ZHANG§, HONG YOU§, YAN LIU§, HAO ZHANG‡, DEZHI SUN§
Departments of ‡Applied Chemistry and §Environment Engineering, Harbin Institute of Technology (HIT), Harbin 150001, People's Republic of China
E-mail: hulijiang@vip.sina.com

Silsesquioxanes (SSO) were synthesized by the hydrolytic condensation of (3-glycidoxypropyl)trimethoxysilane (GPMS). Their structure was characterized by FTIR and NMR (^{1}H, ^{13}C, ^{29}Si), and the molar mass distribution was determined by UV-MALDI-TOF MS. Films were synthesized by adding the stoichiometric amount of ethylenediamine to SSO solutions in ethanol, dip-coating over glass substrates, and curing using an appropriate thermal cycle. The transmittance of the films was measured by UV-VIS-NIR scanning spectrophotometer (SSP); hardness and modulus were determined with the continuous stiffness measurement (CSM) technique of an instrumented-indentation testing (IIT) device. The effect of the substrate on the coating system was analyzed.

1. Introduction

Silsesquioxanes (SSO) have been widely used as precursors of hybrid organic/inorganic polymers, combining the basic elements and structural features of inorganic compounds with those commonly associated with organic compounds [1, 2]. Feher's group [3–5] has worked with silsesquioxanes, focusing on the synthesis of several active catalysts for the polymerization, metathesis and epoxidation of olefins since 1985, and has recently devised methods for synthesizing dendrimers and cube-octameric silsesquioxanes with biologically-active pendant groups. Wallace and Williams *et al*. [6–11] characterized broad molar mass distribution of condensed silsesquioxanes produced from trialkoxysilanes by matrix-assisted ultraviolet laser desorption/ionization time-of-flight mass spectrometry (UV-MALDI-TOF MS). The structures of SSO can be represented by the generic formula, $T_n(OH)_x(OR')_y$ ($n = 1, 2, 3, \ldots$; $x = 0, 1, 2, 3, \ldots$; $y = 0, 1, 2, 3, \ldots$), where $T = RSiO_{1.5-(x+y)/2n}$. Lichtenhan *et al*. [12–14] reported properties and applications of materials modified with polyhedral oligomeric silsesquioxanes (POSS). SSOs have been also used in the formulation of transparent coating films with desirable properties such as abrasion resistance and thermal stability, providing the opportunity to incorporate and release corrosion inhibitors.

In the early 1950s, Brady's group [1] at Dow Corning produced SSO copolymers, phenylsilsesquioxane-alkylsilsesquioxane, with low molecular weights but high hydroxyl functionality, for naval aircraft coatings. Abe and co-workers [15] reported thermal and optical properties of coatings made by polysilsesquioxanes with high molecular weights. They were prepared by the hydrolytic polycondensation of methyltrimethoxysilane and vinyltrimethoxysilane, modified with tetraethoxysilane (TEOS). With a similar preparation based on a sol-gel process, Osborne, Cao and Metroke *et al*. [16–19] researched SSO-epoxy and other hybrid coatings on aluminum alloy substrates for corrosion protection, using wet adhesion testing and electrochemical analyses.

The continuous stiffness measurement (CSM) of an instrumented-indentation testing (IIT) device, a recently developed technique for the determination of mechanical properties of very small thin films, allows a continuous measurement of hardness and elastic modulus during loading [20, 21]. There are a number of reports about this subject; however, most of these studies deal with a hard film coating a soft substrate [22–24].

The purpose of this study was to analyze the application of this new technique to a combination of a soft film and a hard substrate. SSOs synthesized from (3-glycidoxypropyl)trimethoxysilane (SSO-GPMS), were characterized using the same techniques as in our previous studies [25, 26], and were dip-coated on glass substrates together with a stoichiometric amount of

*Author to whom all correspondence should be addressed.

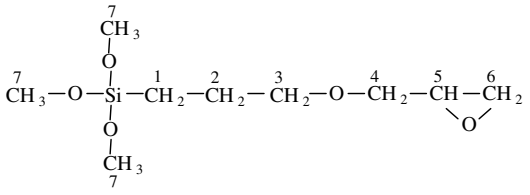

Scheme 1 Structural formula of the commercial GPMS.

ethylenediamine (EDA). Optical and mechanical properties of the films obtained after curing, were determined by UV-VIS-NIR Scanning Spectrophotometry (SSP) and using a Nano Indenter XP (NI XP) with continuous stiffness measurement (CSM).

2. Experimental

2.1. Materials

The structural formula of the commercial (3-glycidoxypropyl)trimethoxysilane (GPMS, Sigma G 1535), is indicated in Scheme 1 (numbers correspond to the assignment of ^{1}H and ^{13}C NMR peaks). Formic acid (HCOOH, 98%), an analytical grade reagent, was used as a catalyst. Ethanol (C_2H_5OH, 99.7%) was used as a solvent. The hardener was ethylenediamine (EDA), an analytical grade reagent. The amount of EDA added to the SSO-GPMS after the hydrolytic condensation was determined as the one giving the maximum glass transition temperature of the cured product.

2.2. Synthesis [25–27]

The hydrolytic condensation of GPMS was carried out in beakers placed in a water bath, using HCOOH in a molar ratio HCOOH/Si = 3. The reaction was performed in three stages. Firstly, plastic films were used to seal the beakers for 3 days, then several small needle-sized holes were made in the films and left for another 3 days, and finally the film was removed and the reaction continued for 4 days. The temperature for every step was held at 35°C. The resulting SSO was diluted with ethanol (molar ratio $Si/C_2H_5OH = 1/4$) and then the theoretical amount of EDA (molar ratio Si/EDA = 4/1), was added. Dip-coating on a glass surface ($76.4 \times 25.2 \times 1.2$ mm) was performed at 270 mm/min. The coated glasses were cured at 80°C for 6 h, followed by 2 h at 120°C.

2.3. Characterization

FTIR spectra were obtained in an Avatar 360 (Nicolet) device, using attenuated total refraction (ATR).

NMR spectroscopy was carried out with a Bruker AV 400 instrument. Syntonic frequencies of ^{1}H, ^{13}C and ^{29}Si were 399.95, 100.58 and 79.45 MHz, respectively; syntonic widths were 4.25, 25.06 and 25.06 kHz; syntonic numbers were 8, 1311 and 3395; pulse angles were 6.5, 2.8 and 7.2 μs; pulse intervals were 9.33, 1.06 and 1.35 s; DMSO-d_6 was used as solvent.

Mass spectra were obtained with a Biflex III UV-MALDI-TOF Mass Spectrometry (Bruker, Billerica), equipped with delayed extraction, a multisample probe, a TOF reflection analyzer, a pulsed nitrogen laser with wavelength 337 nm and pulse width 3 ns, and a linear flight path length of 1 m. The flight tube was evacuated to 10^{-5} Pa. All the measurements were performed in reflectron mode and positive ion detection. The acceleration potential was 19 kV, the reflectron potential 20 kV, the delayed extraction potential was 14.5–17 kV, and the delay times were 50–200 ns; 10–50 single-shot signals were accumulated for each spectrum. Mass calibrations were performed externally, and samples were diluted to 0.25 kg/m^3 and measured in the matrix of a negative ion mode, employing angiotensin II and bovine insulin b-chain (oxidized).

2.4. Measurements of film thickness and transparency

A Hitachi S-570 scanning electron microscope (SEM) device was used to measure the thickness of the film. A Shimadzu UV-3101PC Scanning Spectrophotometer (SSP) device was used to measure the film transparency in a range wavelengths between 190.0 and 3200.0 nm.

2.5. Instrumented-indentation testing

Modulus and hardness of the coating systems were determined using a Nano Indenter XP (MTS Systems Corporation) device, provided with a continuous stiffness measurement (CSM) technique. A triangular pyramid Berkovich indenter was used to fabricate the tip radius. Its indent shape and side view angles were 65.3° and 12.95°, respectively. The Poisson's ratio was 0.3; both the harmonic frame stiffness and the frame stiffness correction were 0 N/m, the loading rate ($\bar{P}/P$) was 0.5 s^{-1}, percent unload in stiffness calculation was 50%, minimum and maximum depths for calculations were 100 and 200 nm, respectively.

3. Results and discussion

3.1. Characterization of SSO-GPMS

Typical Si–O–Si bands of FTIR spectrum at 417–478 and 1122 cm^{-1} were observed. A decrease in the intensity of the band of $SiOCH_3$ groups at 2840 cm^{-1} was also evidenced together with the generation of a broad band at 3420 cm^{-1}, assigned to OH groups from SiOH and from the diol formed through epoxide ring hydrolysis (see Scheme 2) [18].

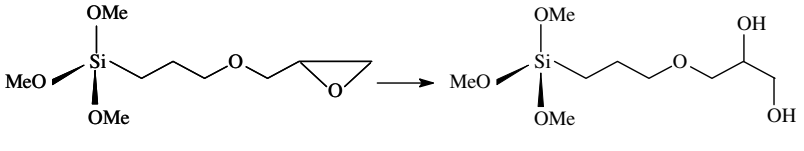

Scheme 2 The epoxide ring opening reaction of GPMS.

The following peaks of ^{1}H NMR spectrum were assigned: 0.485–0.496 ppm (1), 1.577 ppm (2), 3.318–3.467 ppm (3 and 5), 3.069 ppm (4), 3.555–3.690 ppm (4, 7), 3.204–3.287 ppm (5 and 6 after ring-opening reaction), 2.700–2.723 ppm (6, 7), 2.491–2.522 ppm (DMSO-d_6), 3.169 ppm (H_2O) and 6.472 ppm (OH) [18, 28].

The following peaks of ^{13}C NMR spectrum were assigned: 8.400–9.900 ppm (1), 23.288 ppm (2), 72.400–74.610 ppm (3), 70.200–71.460 ppm (4), 50.792 ppm (5), 43.822 ppm (6, 7). In the range from 56.658 to 69.110 ppm, thirteen peaks associated with C─OH resonances after ring-opening of (5) and (6). The DMSO-d_6 signals appeared at $\delta = 38.800$–39.920 and 40.122 ppm; $\delta = 162.38$ ppm corresponds to formic acid (HCOOH). These data are well in an agreement with that of ^{1}H resonances and give complementary information for the characterization of the structure [18, 28].

The ^{29}Si NMR spectrum of the SSO is reported in Fig. 1. The peak at −50.21 ppm is due to Si atoms with only one Si─O─Si bond, the peaks at −58.46 and −59.15 ppm correspond to Si atoms with two Si─O─Si bonds (or to Si atoms with three Si─O─Si bonds in strained cycles), and the peak at −67.53 correspond to Si atoms with three Si─O─Si bonds. Experimental results show the very low condensation degree of the SSO synthesized under the selected experimental conditions.

Fig. 2 shows the UV-MALDI-TOF mass spectra of the SSO. Clusters of peaks correspond to species with *n* Si atoms as indicated in the Figure. A low degree of condensation is apparent from these results.

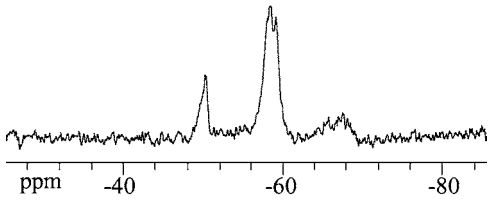

Figure 1 ^{29}Si NMR spectrum (79.45 MHz, DMSO-d_6, 25°C) of SSO-GPMS.

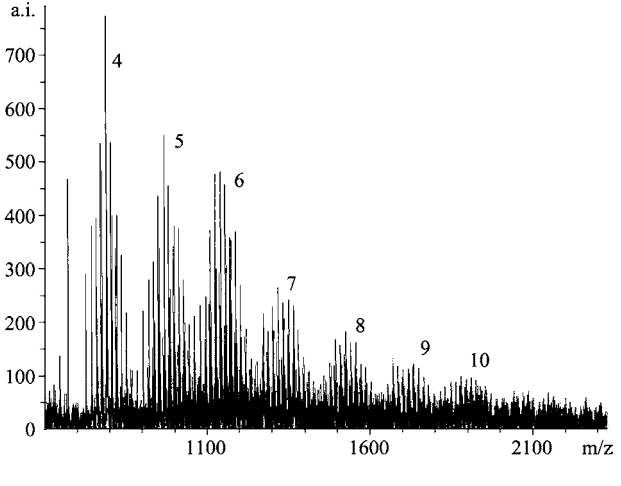

Figure 2 UV-MALDI-TOF mass spectrum (positive ion mode) of SSO-GPMS, in the 745–2265 m/z range.

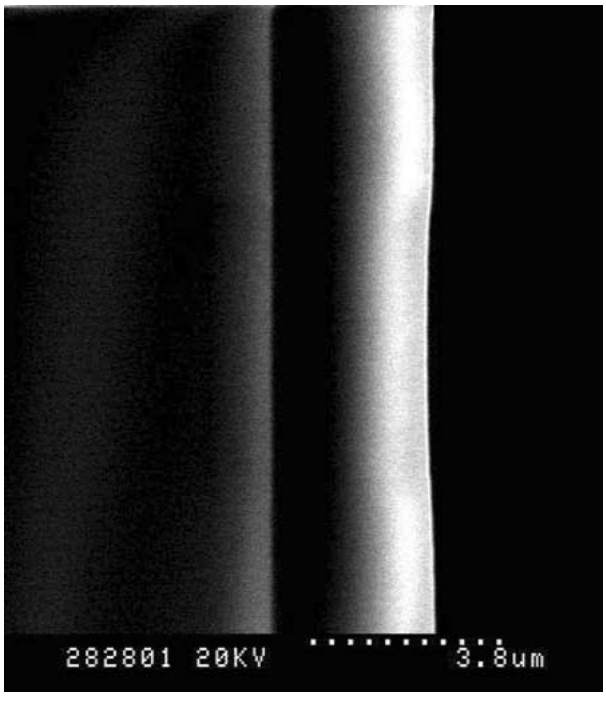

Figure 3 Thickness of a single coated film on the glass, measured by scanning electron microscopy (SEM).

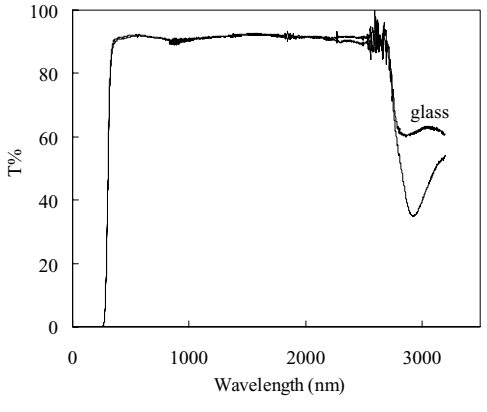

Figure 4 Transmittance of the uncoated glass and a two-side coated glass, measured in the wavelength range: at 190.0–3200.0 nm.

3.2. Testing of properties

3.2.1. Transparency

The transparency of the uncoated glass and a two-sides coated glass (thickness of a single film is 3.5 μm, see Fig. 3), measured at 190.0–3200.0 nm, is shown in Fig. 4. Compared with the transparency (91.48%) of the pure glass illustrated as the top line in Fig. 4, the transparency (91.312%) of the two-sides coated glass is almost the same at the range of visible and near infrared wavelength (345–2500 nm). This means that the film has ideal transparency [29].

3.2.2. Hardness and modulus

Hardness and elastic modulus of coatings on glass substrates were determined with IIT provided with the CSM technique. The plot of hardness vs. displacement for a coating system based on a soft film and a hard substrate, like the SSO-GPMS coating system, can be

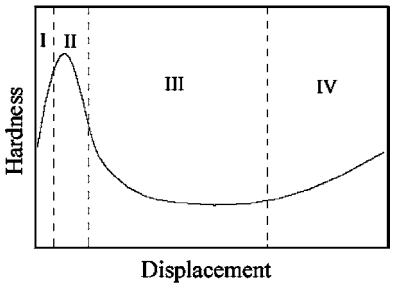

Figure 5 Four regions in a plot of hardness vs. penetration: I. Superficial region; II. Region of the maximum value; III. Region of a constant value; IV. Region showing a substrate effect.

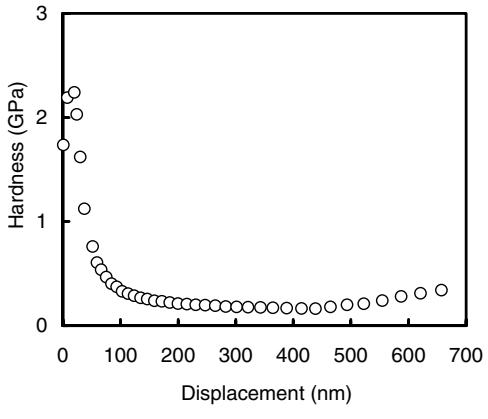

Figure 6 Hardness as a function of penetration.

divided into four regions: superficial region, region of the maximum value, region of a constant value and region showing a substrate effect (see Fig. 5). This description is different from the popular three-region (or layers) explanation for a coating system consisting of a hard coating film and a soft substrate [22, 30]. As seen in Fig. 6, in the first region, hardness increases from zero to a maximum value when increasing the penetration of the indenter. This region extends for approximately 10–15 nm. In the second region, the hardness reaches the maximum value (2.24 GPa) and then decreases. This maximum value is an artifact provoked by the film-surface layer and a pile-up effect [31]. However, sometimes it has been erroneously considered as a basis of the evaluation of the experimental hardness of the films [22]. In the third region, the hardness decreases with higher penetrations to a constant value at indentation depths ranging from 100 to 400 nm. In the last region, the hardness starts to increase again due to the effect of the substrate.

The value of the elastic modulus during loading followed a similar trend described in the four regions mentioned above (see Fig. 7). It initially increases from zero to reach a maximum value (6.13 GPa), then decreases and attains a constant value and finally increases due to the effect of the substrate. The influence of the substrate on the modulus measurement (elastic behavior) is much bigger than in the case of hardness measurement (plastic behavior).

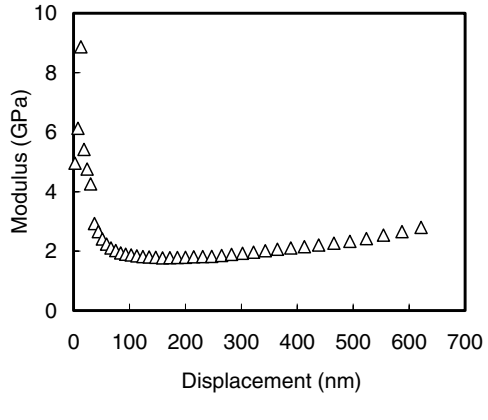

Figure 7 Elastic modulus as a function of penetration.

4. Conclusions

Transparent coating films based on a SSO-GPMS system were obtained using a glass surface as a substrate. Hardness and modulus of the soft coating/hard substrate combination were determined with the continuous stiffness measurement (CSM) of an instrumented-indentation testing device (IIT). The plots of hardness and modulus vs. penetration could be described in a four-region scheme. The influence of the substrate on the modulus measurement (elastic behavior) was much bigger than in the case of hardness measurement (plastic behavior).

Acknowledgement

We acknowledge the financial support of the Department of Science and Technology, The Government of Heilongjiang Province, China.

References

1. B. ARKLES, *MRS Bull.* **26** (2001) 402.
2. D. A. LOY, *MRS Bull.* **May** (2001) 364.
3. F. J. FEHER, D. A. NEWMAN and J. F. WALZER, *J. Amer. Chem. Soc.* **111** (1989) 1741.
4. F. J. FEHER, R. TERROBA and J. W. ZILLER, *Chem. Commun.* (1999) 2153.
5. J. XIAO and F. J. FEHER, *Polym. Mater. Sci. Eng.* **86** (2002) 171.
6. W. E. WALLACE, H. CHEN and R. E. TECKLENBURG, *Rapid. Comm. Mass. Spect.* **15** (2001) 2176.
7. W. E. WALLACE and C. M. GUTTMAN, *J. M. Antonucci, Polym.* **41** (2000) 2219.
8. P. EISENBERG, R. ERRA-BALSELLS, Y. ISHIKAWA, J. C. LUCAS, A. N. MAURI, H. NONAMI, C. C. RICCARDI and R. J. J. WILLIAMS, *Macromolecules* **33** (2000) 1940.
9. R. J. J. WILLIAMS, R. E ERRA-BALSELLS, Y. ISHIKAWA, H. NONAMI, A. N. MAURI and C. C. RICCARDI, *Macromol. Chem. Phys.* **202** (2001) 2425.
10. D. P. FASCE, R. J. J. WILLIAMS, R. ERRA-BALSELLS, Y. ISHIKAWA and H. NONAMI, *Macromolecules* **34** (2001) 3534.
11. P. EISENBERG, R. ERRA-BALSELLS, Y. ISHIKAWA, H. NONAMI, J. C. LUCAS and R. J. J. WILLIAMS, *ibid.* **35** (2002) 1160.
12. R. A. MNATZ, P. F. JONES, K. P. CHAFFEE, J. D. LICHTENHAN and J. W. GILMAN, *Chem. Mater.* **8** (1996) 1250.
13. T. S. HADDAD, H. W. OBVIATE, J. J. SCHWAB, P. T. MATHER, K. P. CHAFFEE and J. D. LICHTENHAN, *Polym. Prep.* **39** (1998) 611.

14. B. XU, B. FU, S. HSIAO, S. PAGOLA, P. STEPHENS, H. WHITE, M. RAFAILOVICH, J. SOKOLOV, P. T. MATHER, H. G. JEON, J. D. LICHTENHAN and J. SCHWAB, *Polym.* **42** (2001) 599.
15. Y. ABE, K. KAGAYAMA, N. TAKAMURA, T. GUNJI, T. YOSHIHARA and N. TAKAHASHI, *J. Non-Cryst. Solids* **261** (2000) 39.
16. Y. J. DU, M. DAMRON, G. TANG and H. ZHENG, *Prog. Org. Coat.* **41** (2001) 226.
17. T. P. CHOU, C. CHANDRASEKARAN, S. J. LIMMER, S. SERAJI Y. WU, M. J. FORBESS, C. NGUYEN and G. Z. CAO, *J. Non-Cryst. Solids* **290** (2001) 153.
18. T. L. METROKE, O. KACHURINA and E. T. KNOBBE, *Prog. Org. Coat.* **44** (2002) 295.
19. O. M. KACHURINA, T. L. METROKE and E. T. KNOBBE, in Proceedings of the Interdisciplinary Workshop: Organic/Inorganic Hybrid Materials, Rohnert Park, CA (2001) p. 4.
20. J. MAIZBENDER, J. M. J. DEN TOONDER, A. R. BALKENEDE and G. DE WITH, *Mater. Sci. Eng.* R **36** (2002) 47.
21. X. LI and B. BHUSHAN, *Mater. Charact.* **48** (2002) 11.
22. M. TABBAL, P. MEREL, M. CHAKER, M. A. EL KHAKANI, E. G. HERBERT, B. N. LUCAS and M. E. O'HERN, *Surf. Coat. Technol.* **116–119** (1999) 452.
23. X. LI, B. BHUSHAN and M. INOUE, *Wear* **251** (2001) 1150.
24. L. HUANG, K. XU, J. LU, B. GUELORGET and H. CHEN, *Diam. Relat. Mater.* **10** (2001) 1448.
25. L. HU, Y. SUN, S. ZHAO and Z. LIU, *Polym. Prepr.* **43** (2002) 1114.
26. L. HU, Y. SUN, S. ZHAO and Z. LIU, in Proceedings of the Interdisciplinary Workshop: Organic/Inorganic Hybrid Materials, Rohnert Park, CA (2001) p. 1.
27. D. P. FASCE, R. J. J. WILLIAMS, F. MECHIN, J. P. PASCAULT, M. F. LLAURO and R. PETIAUD, *Macromolecules* **32** (1999) 4757.
28. D. HOEBBEL, M. NACKEN and H. SCHMIDT, *J. Sol-Gel Sci. Technol.* **12** (1998) 169.
29. R. KASEMANN and H. SCHMIDT, *J. Chem.* **18** (1994) 1117.
30. S. LOGOTHETIDIS, C. CHARITIDIS and P. PATSALAS, *Diam. Relat. Mater.* **11** (2002) 1095.
31. A. BOLSHAKOV, W. C. OLIVER and G. M. PHARR, *Mater. Res. Soc. Symp. Proc.* **436** (1997) 141.

Received 9 January
and accepted 24 September 2003